

3. Vodoraspredelitel'nye sistemy bashennyh gradiren / Fedyayev V. L., Morenko I. V., Molov V. I., Gaynullin R. F. // Shkola-seminar molodyh uchenykh i specialistov akademika RAN V. E. Alemasova «Problemy teplomasoobmena i gidrodinamiki v energomashinostroenii»: Materialy dokladov. Kazan', 2008. P. 170–173.
4. Influences of Cooling Air Face Velocity and Temperature on Dynamic Characteristics of Direct Air-cooled System / Yufeng G., Hua Q., Daren Y., Xiaomin Z. // CSEE Journal. 2008. Vol. 29. P. 22–27.
5. Husick C. California's Otay Mesa selects Niagara Blower WSAC to keep its cool // Modern Power Systems. 2008. Vol. 28, Issue 6. P. 45.
6. Analytical equation for outflow along the flow in a perforated fluid distribution pipe / Liu H., Zong Q., Lv H., Jin J. // PLOS ONE. 2017. Vol. 12, Issue 10. P. e0185842. doi: <https://doi.org/10.1371/journal.pone.0185842>
7. Lee S., Moon N., Lee J. A study on the exit flow characteristics determined by the orifice configuration of multi-perforated tubes // Journal of Mechanical Science and Technology. 2012. Vol. 26, Issue 9. P. 2751–2758. doi: <https://doi.org/10.1007/s12206-012-0721-z>
8. Modeling the Uniformity of Manifold with Various Configurations / Hassan J. M., Mohamed T. A., Mohammed W. S., Alawee W. H. // Journal of Fluids. 2014. Vol. 2014. P. 1–8. doi: <https://doi.org/10.1155/2014/325259>
9. Cherniuk V. V. Metod rozrakhunku napirnykh rozpodilchykh truboprovodiv // Prykladna hidromekhanika. 2008. Issue 3. P. 65–76.
10. Chernyuk V., Orel V. Experimental Verification of a New Method of Calculation for Pressure Distributive Pipelines // Zeszyty Naukowy Politechniki Rzeszowskiej. 2009. Issue 266. P. 27–34.
11. Idel'chik I. E. Spravochnik po gidravlicheskim soprotivleniyam / M. O. Shteynberg (Ed.). 3-e izd., pererab. i dop. Moscow: Mashinostroenie, 1992. 672 p.

З метою інтенсифікації теплообмінних процесів в елементах енергетичного обладнання при мінімальних енерговитратах була розроблена концепція часткового структурування теплообмінної поверхні. Для визначення енергоефективності часткового структурування теплообмінної поверхні при перехідних числах Рейнольдса розглянуто поверхню у вигляді витого гофрування. Часткове вите гофрування за рахунок зміни структури течії дозволяє отримати збільшення конвективної складової теплообміну при помірному зростанні гідравлічних втрат за перехідних режимів течії. На підставі прямого чисельного моделювання формування тривимірної нестационарної структури течії на початковій ділянці труби з витотою гофрованою вставкою при ударному вході і перехідному числі Рейнольдса показано взаємозв'язок збуреної структури неізотермічної течії із значенням інтенсивності теплообміну на поверхні труби. Показано вплив величини температурного напору на швидкість зростання збурень прилежового шару в трубі, в межах якого формуються низькочастотні коливальні процеси потоку, що призводять до збільшення конвективного теплообміну. Досліджено характер течії і зміни гідродинамічних і теплових параметрів всередині гофрованої вставки. Визначено ступінь впливу витотої гофрованої вставки, що не загромождає прохідний переріз труби, на розвиток власних коливань в трубі. Досліджено вплив кута нахилу витого гофрування до осі труби на теплові та гідродинамічні процеси в ній. Отримана інтенсифікація теплообміну (до 20 %) при супутньому зростанні гідравлічних втрат (до 7,5 %) корелює з експериментальними результатами інших авторів при подібних параметрах гофрування в даному діапазоні чисел Рейнольдса

Ключові слова: часткове гофрування, вите гофрування, теплообмін в трубі, інтенсифікація теплообміну, гідравлічний опір

UDC 532.542

DOI: 10.15587/1729-4061.2019.165852

INFLUENCE OF THE FLOW STRUCTURE FORMATION ON HEAT TRANSFER PROCESSES IN TUBES WITH SPIRAL CORRUGATED INSERTS

O. Baskova

Engineer of 1 category*

E-mail: BaskAleksandra@gmail.com

G. Voropaiev

Doctor of Physical and Mathematical Sciences,

Professor, Head of Department*

E-mail: voropaiev.gena@gmail.com

*Department of Hydrobionics and

Boundary Layer Control

Institute of Hydromechanics National Academy of

Sciences of Ukraine

Zhelyabova str., 8/4, Kyiv, Ukraine, 03680

1. Introduction

Energy efficiency of heat transfer equipment with fuel shortage is a key issue for the power industry. To increase

the rate of heat transfer processes, there are several methods, centered on changing the flow structure by acting on it from the outside or changing the shape of the heat transfer surface. The latter method is less power-consuming, but its

energy efficiency varies widely depending on the structure formation geometry of the heat transfer surface and flow conditions. There are not so many effective passive methods, taking into account resource expenditures. This fact led to the development and study of partial corrugation of the heat transfer surface, which allows increasing the heat transfer rate several times with a moderate increase in the cost of coolant pumping. In addition, partial corrugation has minimal material consumption, compared with the majority of methods of heat transfer surface development. These characteristics determine the possibility of using this passive method of heat transfer enhancement in nuclear power engineering, heat exchangers design, chemical industry, etc. [1].

2. Literature review and problem statement

Structure formation of the heat transfer surface in the form of the corrugations of various geometric parameters has become particularly active in the last thirty years. A number of studies, in particular [2–9], are devoted to the analysis of heat transfer enhancement and the accompanying growth of friction loss.

In [2], the results of experimental studies of the flow structure and friction loss in a plane channel with the introduction of sinusoidal symmetric and asymmetric corrugation under the laminar flow regime are presented. The authors [3] continue the study of the flow structure with asymmetric corrugation of the heat transfer surface of the channel, while evaluating the degree of heat transfer enhancement and friction loss. The numerical experiment was carried out in laminar and transient flow regimes in the range of Prandtl numbers $Pr=1..9.4$. A rather large increase in heat transfer rate was obtained compared to a plain channel (up to 3 times), but due to a very large increase in friction loss (up to 10 times), which is probably due to a loss of flow stability and transition to a turbulent flow regime. In [4, 5], friction loss and heat transfer in channels of complex three-dimensional geometry are considered. Experimental studies were carried out with a wide variation of pitches of corrugation surfaces forming the channel walls and in the range of Reynolds numbers $Re=400..6,000$. The increase in heat transfer rate up to 2 times with an increase in the guide corrugation pitch from 30° to 75° with a corresponding increase in friction loss up to 5 times is shown.

Spiral surface corrugation of the tube of various geometric parameters $w/a=14..44$, where w – length, a – corrugation wavelength amplitude, in a wide range of Reynolds $Re=2,000..90,000$ and Prandtl numbers $Pr=2.5..100$ is studied in [6]. Heat transfer enhancement up to 2.5 times is obtained with an increase in friction loss up to 3 times. The values of heat transfer enhancement in this work are consistent with the data of [7, 8] for spiral corrugation of similar geometric parameters $w/a=16.8..36$ in the corresponding range of Reynolds and Prandtl numbers.

In the numerical study by the authors of [9], flow simulation in a tube with spiral corrugation in the same range of the ratio of the corrugation wave amplitude to the length ($w/a=12.5..50$) with Reynolds numbers: $Re=5,000; 10,000$ is considered. The dependence of the energy efficiency parameter $E=(Nu/Nu_0)/(f/f_0)^{1/3}$ of the corrugated surface on the wave amplitude and length is obtained. Friction loss with increasing corrugation amplitude increases over the entire wavelength range. While the heat transfer rate has

a clear extremum in the region of medium wavelengths and amplitudes of the corrugation, which provides the maximum energy efficiency $E=1.57$ with $Re=5,000$ with $w/a=8..14$. An increase in the Reynolds number leads to a decrease in energy efficiency over the entire range of geometric parameters considered, but the energy efficiency coefficient E remains greater than unity.

The reviewed papers are devoted to the study of flow structure and prove the energy efficiency of fully corrugated surfaces. The energy efficiency of partial structure formation of the heat transfer surface is not studied. However, it is periodic corrugation that allows to significantly reduce the cost of coolant pumping while maintaining a high level of heat transfer enhancement, which prompted a series of numerical experiments.

3. The aim and objectives of the study

The aim of the study is to assess the energy efficiency of partial spiral corrugation of the tube surface.

To achieve this aim, the following objectives were set:

- to investigate the flow structure in the initial section of the tube with spiral corrugated inserts of the given parameters;
- to assess the degree of influence of the structured insert on heat transfer processes and to compare the thermal and hydraulic characteristics of flows for different types of spiral corrugation and plain tube.

4. Problem statement and methodology of numerical experiment

The flow of water in the initial section of the tube with various corrugated inserts shown in Fig. 1 is considered. The flow in tubes with a radius of 35 mm consisting of an inlet branch (length 1,500 mm), a corrugated insert (length 300 mm) and an outlet branch (length 1,360 mm) is investigated. The wavelength of one corrugation was 20 mm, height – 6 mm. Depending on the pitch of spiral corrugation to the tube axis, the shape of the section changed. At a corrugation pitch of 80° (corrugation pitch 40 mm), the cross section of the corrugated tube takes an ellipsoid shape (Fig. 1, *a*) and has an area of 0.00454235 m^2 , 1.18 times larger than in the plain tube. The corrugation pitch of 70° with respect to the tube axis (corrugation pitch 80 mm) forms the section shown in Fig. 1, *b* with an area of 0.00454188 m^2 .

The inner flow of a viscous incompressible heat-conducting fluid is described by the system of non-stationary three-dimensional Navier-Stokes, continuity and energy equations (1)–(3):

$$\rho \frac{\partial u_i}{\partial t} + \rho \frac{\partial(u_j u_i)}{\partial x_j} = - \frac{\partial p}{\partial x_i} + \frac{\partial}{\partial x_j} \left(\mu \left(\frac{\partial u_i}{\partial x_j} + \frac{\partial u_j}{\partial x_i} \right) \right), \quad (1)$$

$$\frac{\partial u_j}{\partial x_j} = 0, \quad (2)$$

$$\frac{\partial T}{\partial t} + u_j \frac{\partial T}{\partial x_j} = a \left(\frac{\partial^2 T}{\partial x_1^2} + \frac{\partial^2 T}{\partial x_2^2} + \frac{\partial^2 T}{\partial x_3^2} \right) + \frac{\mu}{2c_p \rho} \left(\frac{\partial u_i}{\partial x_j} + \frac{\partial u_j}{\partial x_i} \right)^2, \quad (3)$$

where μ is the dynamic viscosity coefficient depending on temperature, obtained from table values [10] for the temperature range $T=5^\circ\dots60^\circ$:

$$\mu = 1,88 \cdot 10^{-4} (1,48 \cdot 10^{-3} \cdot T^2 - T + 171,36),$$

$$a = \frac{\lambda}{c_p \rho}$$

is the thermal diffusivity coefficient. Such problem statement allows revealing the appearance of disturbances in the flow and tracing their downstream development from the inlet section.

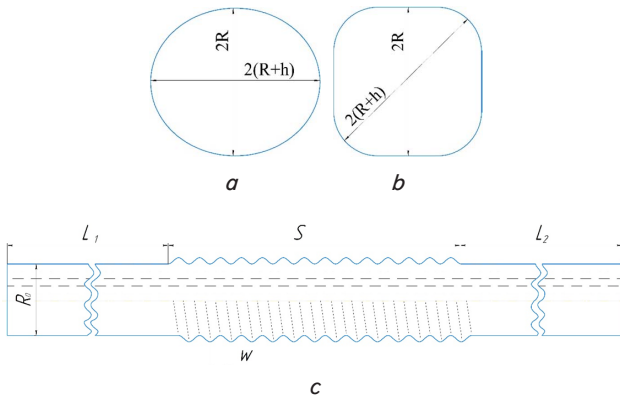


Fig. 1. Tube geometry: *a* – corrugation pitch of 80°; *b* – corrugation pitch of 70°; *c* – scheme of the tube under study

The problem was solved numerically using the ANSYS Fluent codes under the following conditions. A constant flow rate and temperature of the coolant $U_0=0.1$ m/s ($Re=5.3 \cdot 10^3$, determining the size – diameter of the plain tube section) and temperature $T_0=333$ K were set at the inlet. On the wall – adhesion conditions and constant temperature $T_w=283$ K. Simulation was carried out using the Pressure-Based algorithm in combination with the pressure-velocity coupling algorithm – Semi-Implicit Method for Pressure-Linked Equations. Difference grids were constructed in such a way that the smallest cell size was in the wall area. The smallest cell size was determined by the Reynolds number and local thicknesses of the dynamic and thermal boundary layers and corresponded to the value of the parameter $h^+=(u^* \cdot \Delta r)/\nu=0.4$ (Fig. 2). Toward the wall, the grid thickened. The number of grid cells was about 5,200 thousand.

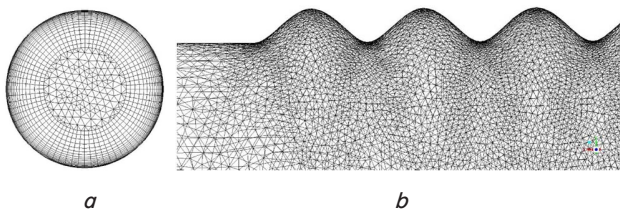


Fig. 2. Fragment of the computational grid: *a* – cross section; *b* – corrugated section, side view

The time step was determined by the Courant number and selected in such a way that the condition: $Co < 2$ holds.

5. Changes in the flow structure and heat transfer rate in the plain tube and tubes with the corrugated insert

At the shock entry of the tube, the calculation results show the formation of dynamic and thermal boundary layers. At the same time, on the tube section $x/d < 8.5$, the flow has an ordered layered nature, disturbances of the flow parameters are present, but very small compared with the corresponding average values, as shown by the trajectories of the tag particles in Fig. 3 with $x/d=2$. The phase portrait of the tag particles shown in Fig. 3 means the coordinates of the intersection point in each cross section of the tube with a step corresponding to the dimensions of the computational grid.

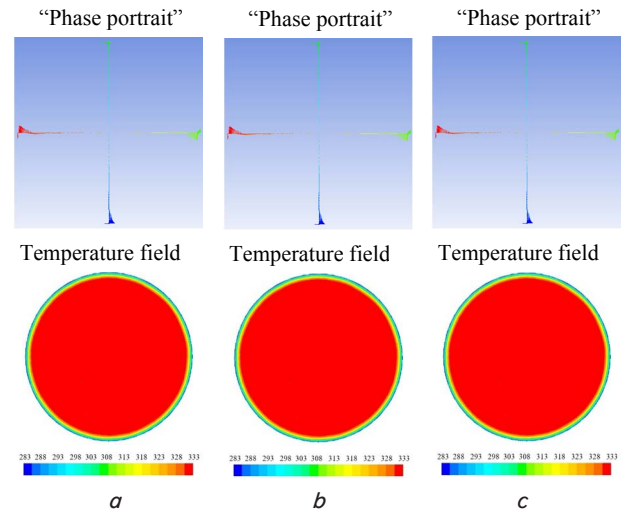


Fig. 3. Phase portraits of tag particles and temperature field in the plain tube and tube with the corrugated insert in the inlet branch with $x/d=2$: *a* – plain tube; *b* – tube with a corrugation pitch of 80°; *c* – tube with a corrugation pitch of 70°

The temperature fields (Fig. 3) demonstrate the unperturbed flow core and a thin boundary layer δ_{th} , which is approximately 2.5 mm. At the same time, the dynamic boundary layer is much thicker $\delta_{dl}=5$ mm, which is due to the values of the Prandtl numbers much greater than 1.

Downstream ($8.5 < x/d < 20$), there is an increase in velocity perturbations, demonstrated by the phase portrait of intersection of the trajectories of tag particles of consecutive sections of the tube (Fig. 4).

Velocity perturbations in the wall region lead to deformation of the temperature boundary layer along the tube perimeter, which is not observed in the flows at a constant temperature with the corresponding Reynolds numbers. This change can be explained by the substantial non-isothermality of the flow in the wall region ($\Delta T=50$ K), which with “cold” tube walls ($T_w=283$ K, $T_0=333$ K) causes a negative viscosity gradient along the normal to the tube wall. At the same time, the oscillations generated on this tube section remain regular, have small amplitudes and do not lead to significant changes in the values of heat flows and friction stresses on the tube surface [11]. Further downstream, the disturbances increase in amplitude and wavelength, quickly becoming disordered with the considered Reynolds number. Along the perimeter of the tube, there is a substantial aperiodicity of the transverse velocity component in the wall re-

gion, which is also manifested in the form of perturbations of the temperature boundary layer (Fig. 4). The flow structures in the plain tube (Fig. 4, *a*) and in the tube with the insert (Fig. 4, *b, c*) up to this insert almost coincide and have the same range of thermal and hydraulic parameters, which indirectly confirms the correctness of independent calculations.

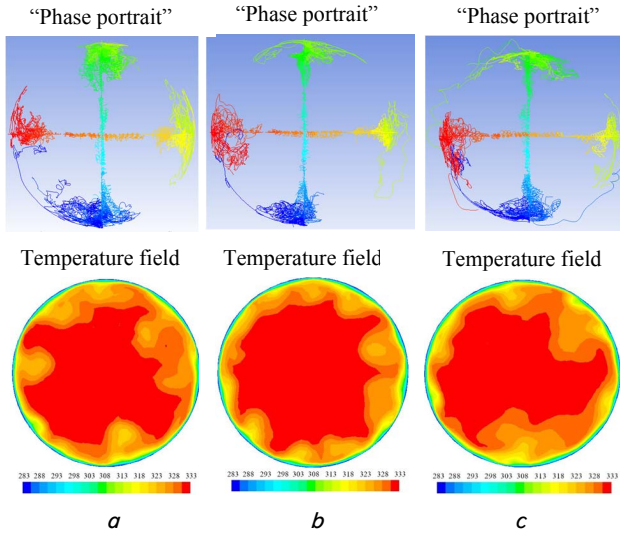


Fig. 4. Phase portraits of tag particles and temperature field in the plain tube and tube with the corrugated insert in the inlet branch with $x/d=20$: *a* – plain tube; *b* – tube with a corrugation pitch of 80° ; *c* – tubes with a corrugation pitch of 70°

With the considered Reynolds number in the tube section ($10 < x/d < 14$), the intensity of the disturbances increases dramatically, which is demonstrated by changes in the maximum values of the normal velocity component in the tube sections (Fig. 5). The results obtained confirm natural development of perturbations in the tube, similar to transition processes in the boundary layer on the plate.

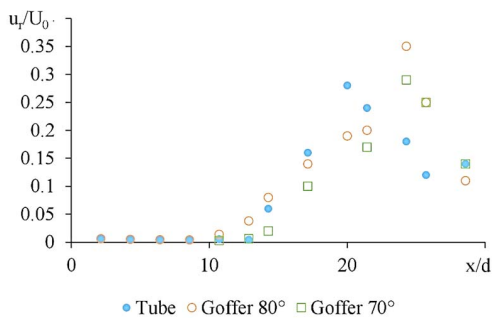


Fig. 5. Variation of dimensionless maximum (over the cross section) values of normal velocity components along the tube length

In the region of the corrugated insert with $21 \leq x/d \leq 25$, where the development of natural flow perturbations in the wall region is distorted by disturbances generated by the spiral surface of the corrugated insert, disturbance amplitudes reach the maximum values.

Once in the corrugation grooves, flow particles are involved in the rotational motion, moving forward, which is demonstrated by the phase portrait of particle trajectories (Fig. 6). Convective heat transfer processes involve addi-

tional volumes of fluid, which contributes to heat transfer enhancement. The flow core remains practically unperturbed. In the wall region, the trajectories of tag particles in the considered area differ somewhat depending on the type of tube surface. Thus, in the plain tube (Fig. 6, *a*), the phase portrait shows intense oscillations along the longitudinal axis, covering a larger area compared to the other tubes under consideration. At the same time, along the corrugated section (Fig. 6, *b, c*), the tracks of the particles in the wall region, along with the rectilinear motion, demonstrate the presence of spiral movement along the helical surface of the corrugations. In this case, the temperature field near the tube surface is significantly perturbed, which is reflected in the heat transfer rate in comparison with the plain tube.

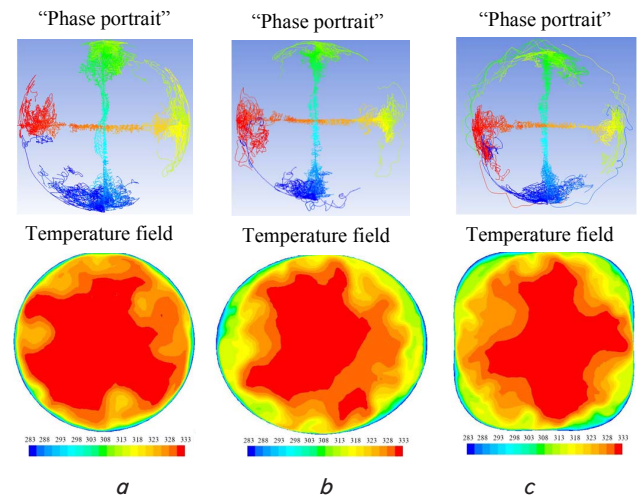


Fig. 6. Phase portraits of tag particles and temperature field in the region of the corrugated insert in tubes of various configurations with $x/d=24$: *a* – plain tube; *b* – tube with a corrugation pitch of 80° ; *c* – tube with a corrugation pitch of 70°

At the outlet branch with $25 \leq x/d \leq 45$, the region of the unperturbed isothermal flow core is significantly reduced. This is demonstrated both by the total phase portrait of the trajectories of tag particles in the tube cross section $x/d=45$ and by the temperature fields in the plain tube (Fig. 7, *a*) and in tubes with partial corrugation (Fig. 7, *b, c*).

Mixing of flows in the wall area is affected by the spiral corrugation pitch. At a spiral corrugation pitch of 80° (Fig. 7, *b*), the trajectories of the particles that fell into the groove during passing the corrugation spiral deviate from the longitudinal direction by no more than 160° . While in the corrugated insert with a pitch of 70° (Fig. 7, *c*), the particles describe an almost complete circle as they move down the spiral. Thus, the introduction of spiral corrugated inserts with the considered pitches leads to more intense mixing.

The spectral analysis of pressure pulsations at the point behind the corrugated insert showed a trend to narrowing of the frequency range of pressure pulsations in the plain tube. At the same time, there is a greater filling of the spectrum in the low-frequency region (Fig. 8, *a*), caused by intensification of large-scale perturbations.

From the obtained spectral characteristics, it follows that the tubes with the corrugated insert (Fig. 8, *b*) in the frequency range up to 1 Hz generate more intense perturba-

tions than in the plain tube, as indicated by large values of spectral power.

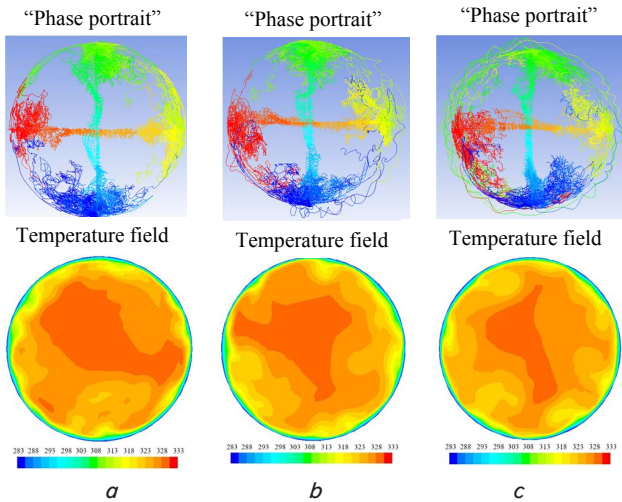


Fig. 7. Phase portraits of tag particles and temperature field in the area of the outlet branch in tubes of various configurations with $x/d=45$: *a* – plain tube; *b* – tube with a corrugation pitch of 80° ; *c* – tube with a corrugation pitch of 70°

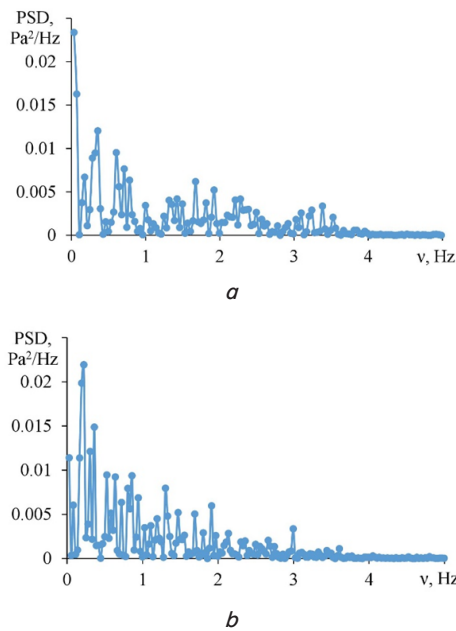


Fig. 8. Frequency spectra of pressure pulsations with $Re=5300$: *a* – plain tube; *b* – tube with a corrugation pitch of 70°

6. Comparative analysis of heat transfer rate and friction loss for tubes with spiral corrugated surfaces and plain tubes

In the zone of the corrugated insert, a substantial increase in heat transfer rate and friction stress values occurs in the ridges of the corrugations, where the thickness of dynamic and thermal boundary layers is minimal (Fig. 9). The development of disturbances leads to inhomogeneous distributions of friction stress and heat flux density, which is

indicated by spots along the forming ridges (Fig. 9, *a, b* and Fig. 10, *a, b*). Once in the corrugation ridge, the disturbed flow is divided. Part of it goes into the groove, forming a vortex structure, which is indicated by areas with negative friction stress values. In this case, the pitch of spiral corrugation practically does not affect friction stress values on the surface.

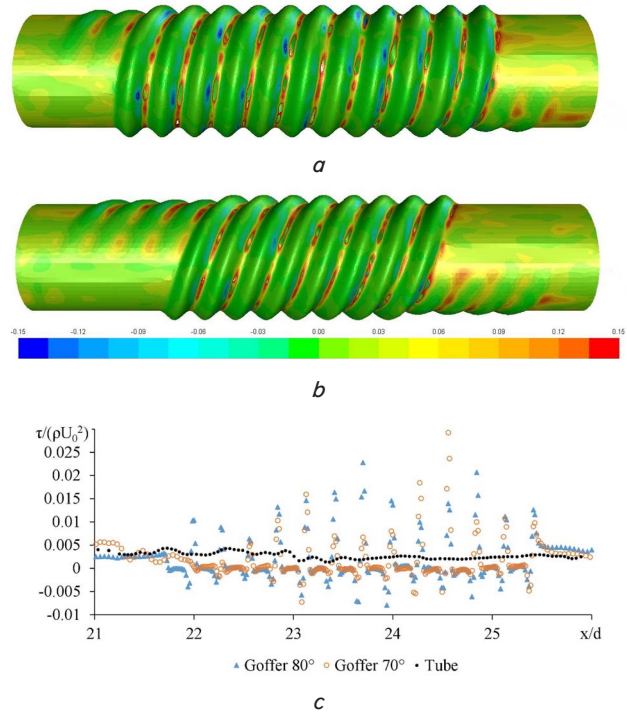


Fig. 9. Friction stress on the corrugated section of tubes of various configurations: *a* – friction stress (Pa) in a tube with a corrugation pitch of 80° ; *b* – friction stress (Pa) in a tube with a corrugation pitch of 70° ; *c* – dimensionless friction stress

In general, the presence of a vortex structure leads to a decrease in friction in the corrugated section, which allows reducing the friction loss (Fig. 9, *c*). In this case, the vortex structure promotes the mixing of liquid from the low-temperature region of the groove into the hotter region in the flow core, which contributes to the enhancement of convective heat transfer (Fig. 10).

At this time, another part of the flow is carried away downstream, contacting only with the corrugation ridge, reducing the thickness of the boundary layer on it. At the same time, the values of τ_x (Fig. 9) and heat flux density (Fig. 10) decrease with decreasing corrugation pitch. In addition, as a result of the influence of long-wave natural flow disturbances, a local increase in friction stress (Fig. 9, *c*) and heat transfer enhancement (Fig. 10, *c*) occur not only on the ridges, but also in the grooves of the corrugations. Thereby destroying small stagnant zones in the grooves of the corrugations at large pitches of spiral corrugation.

When dimensionless perturbation values of the transverse velocity components exceed $u_v/U_o=0.05$ (Fig. 5), it can be assumed that a transition boundary layer is formed on the tube surface. However, a noticeable change in heat transfer is not observed. At the same time, further development of disturbances occurs quite rapidly, and the maximum values of dimensionless velocity u_v/U_o increase several times at a

distance of $(5...7)d$. Starting from this area, a significant increase in heat transfer rate is recorded compared with the laminar flow regime.

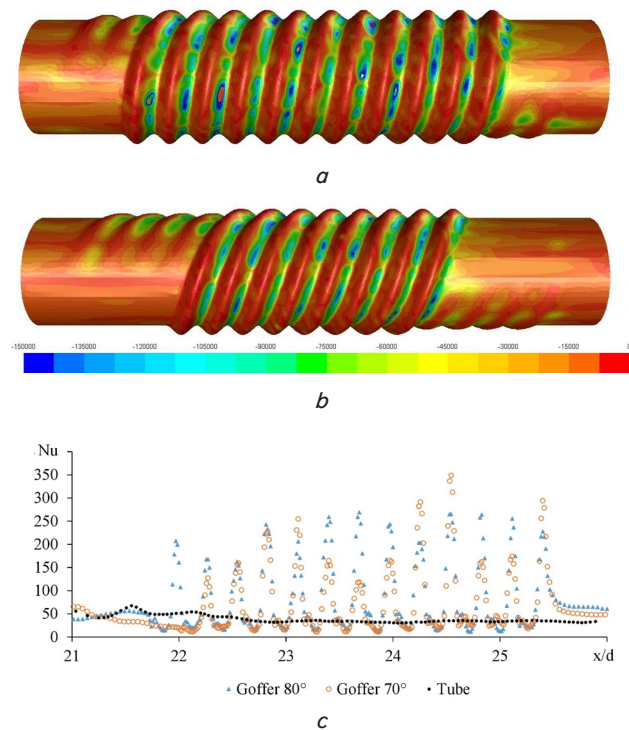


Fig. 10. Heat flux density and Nusselt number values in the corrugated section of tubes of various configurations: *a* – heat flux density (W/m^2) in a tube with a corrugation pitch of 80° ; *b* – heat flux density (W/m^2) in a tube with a corrugation pitch of 70° ; *c* – dimensionless heat transfer values

Heat transfer rate in the area of corrugation and the outlet branch with a slight difference in friction loss values depends on the pitch of spiral corrugation. Thus, the corrugation with a pitch of 80° increases the heat transfer rate by 19 %, while at a corrugation pitch of 70° – by 14 % compared to the plain tube with the same Reynolds number (Table 1):

Table 1

Influence of the corrugated surface geometry on the heat transfer rate and friction loss

Corrugation pitch	$\Delta P/\Delta P_{pl}$	Nu/Nu_{pl}
80°	1.071	1.19
70°	1.074	1.14

The insignificant difference in heat transfer rate is caused by a large number of full corrugation spirals with a larger value of the corrugation pitch, as well as a smaller slip of the flow over the corrugation.

The obtained results are compared with the experimental data of the authors [6, 7], where the results of measurements of friction loss and heat fluxes in spiral corrugated tubes with the following geometrical parameters and Reynolds number $Re=5\cdot 10^3$ are presented. Corrugated surfaces with dimensionless corrugation wavelengths $w/d=0.3; 0.4; 0.6$ (in this study 0.29) and corrugation amplitudes $h/d=0.03$ (in this study 0.086) are investigated. An increase in heat

transfer rate in comparison with the plain tube in the range $Nu/Nu_{pl}=1.1...1.3$ is obtained, but the connection with the wave change is not observed in these results. The obtained heat transfer enhancement in this study is comparable to these values. While friction loss in corrugated tubes was significantly higher compared to the plain tube and amounted to $\Delta P/\Delta P_{pl}=1.2...1.4$, which is significantly higher than the values obtained in this study.

7. Discussion of the results of numerical flow simulation in plain tubes and tubes with corrugated inserts

Based on the numerical simulation, the features of formation of the vortex flow structure in the initial section of the tube with the limiting transition Reynolds number were revealed – the appearance and development of perturbations of finite amplitudes, their influence on heat transfer processes:

- on the tube section $x/d < 8.5$, the flow has an ordered layered character, perturbations are small compared with the corresponding average values of flow parameters;
- with $8.5 \leq x/d \leq 21$, an increase in disturbances and deformation of the boundary layer along the tube perimeter are observed. Transients and a significant increase in heat transfer rate in the flow are recorded at a distance of $(15...22)$ from the tube inlet, where the value of the dimensionless longitudinal velocity component u_r/U_o exceeds 0.05;
- in the corrugation area $21 \leq x/d \leq 25$, natural disturbances undergo distortions under the influence of disturbances generated by the corrugated insert. The distribution of friction stress and heat flux density is non-uniform around the tube perimeter;
- in the wake of the corrugation $x/d \geq 25$, there is an intense non-uniform growth of the boundary layer thickness along the tube perimeter and the region of unperturbed flow in the flow core decreases significantly, which leads to enhancement of the convective component of heat transfer.

Thus, with the considered Reynolds number in the initial section of the tube, introduction of the spiral corrugated insert of the considered geometric parameters changed the flow structure and the course of its natural development, which led to an increase in the rate of convective heat transfer. At the same time, in contrast to the fully corrugated surface, studied by the authors [2–9], partial development of the heat transfer surface made it possible to significantly reduce friction loss while maintaining the heat transfer value.

However, a decrease in the temperature head with the given Reynolds number can significantly reduce the energy efficiency of this method of passive heat transfer enhancement in the initial section of the tube of a fixed length due to transition delay and decrease in the rate of low-frequency oscillatory processes in the flow.

In this regard, the appropriate continuation of this research direction will be to study the effect of spiral corrugation on friction loss and heat transfer rate with an increase in the number of corrugations per unit length while maintaining the pitch in a wider range of transition Reynolds numbers and temperature head values.

8. Conclusions

1. The features of generation and development of vortex formations and their influence on the rate of heat transfer

processes in the initial section of the plain tube and their change in tubes with spiral corrugated inserts of given parameters are studied numerically.

2. The length of the laminar section before the appearance of finite disturbances with the given Reynolds number and temperature head, the growth rate of disturbances and their modification on the corrugated tube section, which leads to sharp oscillations of friction stress values and the corresponding heat transfer rate values are determined.

3. The introduction of corrugated inserts of the considered geometry with the specified Reynolds number and temperature head value allowed enhancing heat transfer compared to the plain tube up to 20 % with an increase in the heat transfer surface area to 4.7 %. Related friction loss increased by 7.5 %.

4. A change in the pitch of spiral corrugation to the tube axis while maintaining the flow area of the tube slightly increases the heat transfer rate by up to 5 % with an increase in the pitch from 70° to 80° with a negligible change in friction loss.

References

1. Mitrofanova O. V. *Gidrodinamika i teploobmen zakruchennykh potokov v kanalah yaderno-energeticheskikh ustanovok*. Moscow: FIZMATLIT, 2010. 288 p.
2. Experimental study of fluid flow in the entrance of a sinusoidal channel / Oviedo-Tolentino E, Romero-Méndez R., Hernández-Guerrero A., Girón-Palomares B. // *International Journal of Heat and Fluid Flow*. 2008. Vol. 29, Issue 5. P. 1233–1239. doi: <https://doi.org/10.1016/j.ijheatfluidflow.2008.03.017>
3. Heat transfer enhancement by flow bifurcations in asymmetric wavy wall channels / Guzmán A. M., Cárdenas M. J., Urzúa F. A., Araya P. E. // *International Journal of Heat and Mass Transfer*. 2009. Vol. 52, Issue 15-16. P. 3778–3789. doi: <https://doi.org/10.1016/j.ijheatmasstransfer.2009.02.026>
4. Investigation of flow and heat transfer in corrugated passages – I. Experimental results / Stasiek J., Collins M. W., Ciofalo M., Chew P. E. // *International Journal of Heat and Mass Transfer*. 1996. Vol. 39, Issue 1. P. 149–164. doi: [https://doi.org/10.1016/s0017-9310\(96\)85013-7](https://doi.org/10.1016/s0017-9310(96)85013-7)
5. Ciofalo M., Stasiek J., Collins M. W. Investigation of flow and heat transfer in corrugated passages – II. Numerical simulations // *International Journal of Heat and Mass Transfer*. 1996. Vol. 39, Issue 1. P. 165–192. doi: [https://doi.org/10.1016/s0017-9310\(96\)85014-9](https://doi.org/10.1016/s0017-9310(96)85014-9)
6. Vicente P. G., García A., Viedma A. Experimental investigation on heat transfer and frictional characteristics of spirally corrugated tubes in turbulent flow at different Prandtl numbers // *International Journal of Heat and Mass Transfer*. 2004. Vol. 47, Issue 4. P. 671–681. doi: <https://doi.org/10.1016/j.ijheatmasstransfer.2003.08.005>
7. Zimparov V. D., Vulchanov N. L., Delov L. B. Heat transfer and friction characteristics of spirally corrugated tubes for power plant condensers – 1. Experimental investigation and performance evaluation // *International Journal of Heat and Mass Transfer*. 1991. Vol. 34, Issue 9. P. 2187–2197. doi: [https://doi.org/10.1016/0017-9310\(91\)90045-g](https://doi.org/10.1016/0017-9310(91)90045-g)
8. Vulchanov M. L., Zimparov V. D., Delov L. B. Heat transfer and friction characteristics of spirally corrugated tubes for power plant condensers – 2. A mixing-length model for predicting fluid friction and heat transfer // *International Journal of Heat and Mass Transfer*. 1991. Vol. 34, Issue 9. P. 2199–2206. doi: [https://doi.org/10.1016/0017-9310\(91\)90046-h](https://doi.org/10.1016/0017-9310(91)90046-h)
9. Hærvig J., Condra T., Sørensen K. Numerical Investigation of Single-phase Fully Developed Heat Transfer and Pressure Loss in Spirally Corrugated Tubes // *Proceedings of the 56th Conference on Simulation and Modelling (SIMS 56)*. Linköping University, 2015. P. 391–397. doi: <https://doi.org/10.3384/ecp15119391>
10. Rivkin S. L., Aleksandrov A. A. *Termodinamicheskie svoystva vody i vodyanogo para*. izd. 2-e, pererab. i dop. Moscow: Energoatomizdat, 1984. 80 p.
11. Baskova A., Voropayev G. The structure of the vortex nonisothermal flow at the initial section of the pipe with transient Reynolds numbers // *Hydrodynamics and acoustics*. 2018. Vol. 1, Issue 2. P. 117–131. doi: <https://doi.org/10.15407/jha2018.02.117>